Measurement of Non-Random Event-by-Event Fluctuations of Average Transverse Momentum in $\sqrt{s_{NN}} = 200$ GeV Au+Au and p+p Collisions

S.S. Adler,[5] S. Afanasiev,[17] C. Aidala,[5] N.N. Ajitanand,[43] Y. Akiba,[20,38] J. Alexander,[43] R. Amirikas,[12] L. Aphecetche,[45] S.H. Aronson,[5] R. Averbeck,[44] T.C. Awes,[35] R. Azmoun,[44] V. Babintsev,[15] A. Baldisseri,[10] K.N. Barish,[6] P.D. Barnes,[27] B. Bassalleck,[33] S. Bathe,[30] S. Batsouli,[9] V. Baublis,[37] A. Bazilevsky,[39,15] S. Belikov,[16,15] Y. Berdnikov,[40] S. Bhagavatula,[16] J.G. Boissevain,[27] H. Borel,[10] S. Borenstein,[25] M.L. Brooks,[27] D.S. Brown,[34] N. Bruner,[33] D. Bucher,[30] H. Buesching,[30] V. Bumazhnov,[15] G. Bunce,[5,39] J.M. Burward-Hoy,[26,44] S. Butsyk,[44] X. Camard,[45] J.-S. Chai,[18] P. Chand,[4] W.C. Chang,[2] S. Chernichenko,[15] C.Y. Chi,[9] J. Chiba,[20] M. Chiu,[9] I.J. Choi,[52] J. Choi,[19] R.K. Choudhury,[4] T. Chujo,[5] V. Cianciolo,[35] Y. Cobigo,[10] B.A. Cole,[9] P. Constantin,[16] D.G. d'Enterria,[45] G. David,[5] H. Delagrange,[45] A. Denisov,[15] A. Deshpande,[39] E.J. Desmond,[5] O. Dietzsch,[41] O. Drapier,[25] A. Drees,[44] R. du Rietz,[29] A. Durum,[15] D. Dutta,[4] Y.V. Efremenko,[35] K. El Chenawi,[49] A. Enokizono,[14] H. En'yo,[38,39] S. Esumi,[48] L. Ewell,[5] D.E. Fields,[33,39] F. Fleuret,[25] S.L. Fokin,[23] B.D. Fox,[39] Z. Fraenkel,[51] J.E. Frantz,[9] A. Franz,[5] A.D. Frawley,[12] S.-Y. Fung,[6] S. Garpman,[29,*] T.K. Ghosh,[49] A. Glenn,[46] G. Gogiberidze,[46] M. Gonin,[25] J. Gosset,[10] Y. Goto,[39] R. Granier de Cassagnac,[25] N. Grau,[16] S.V. Greene,[49] M. Grosse Perdekamp,[39] W. Guryn,[5] H.-Å. Gustafsson,[29] T. Hachiya,[14] J.S. Haggerty,[5] H. Hamagaki,[8] A.G. Hansen,[27] E.P. Hartouni,[26] M. Harvey,[5] R. Hayano,[8] X. He,[13] M. Heffner,[26] T.K. Hemmick,[44] J.M. Heuser,[44] M. Hibino,[50] J.C. Hill,[16] W. Holzmann,[43] K. Homma,[14] B. Hong,[22] A. Hoover,[34] T. Ichihara,[38,39] V.V. Ikonnikov,[23] K. Imai,[24,38] D. Isenhower,[1] M. Ishihara,[38] M. Issah,[43] A. Isupov,[17] B.V. Jacak,[44] W.Y. Jang,[22] Y. Jeong,[19] J. Jia,[44] O. Jinnouchi,[38] B.M. Johnson,[5] S.C. Johnson,[26] K.S. Joo,[31] D. Jouan,[36] S. Kametani,[8,50] N. Kamihara,[47,38] J.H. Kang,[52] S.S. Kapoor,[4] K. Katou,[50] S. Kelly,[9] B. Khachaturov,[51] A. Khanzadeev,[37] J. Kikuchi,[50] D.H. Kim,[31] D.J. Kim,[52] D.W. Kim,[19] E. Kim,[42] G.-B. Kim,[25] H.J. Kim,[52] E. Kistenev,[5] A. Kiyomichi,[48] K. Kiyoyama,[32] C. Klein-Boesing,[30] H. Kobayashi,[38,39] L. Kochenda,[37] V. Kochetkov,[15] D. Koehler,[33] T. Kohama,[14] M. Kopytine,[44] D. Kotchetkov,[6] A. Kozlov,[51] P.J. Kroon,[5] C.H. Kuberg,[1,27] K. Kurita,[39] Y. Kuroki,[48] M.J. Kweon,[22] Y. Kwon,[52] G.S. Kyle,[34] R. Lacey,[43] V. Ladygin,[17] J.G. Lajoie,[16] A. Lebedev,[16,23] S. Leckey,[44] D.M. Lee,[27] S. Lee,[19] M.J. Leitch,[27] X.H. Li,[6] H. Lim,[42] A. Litvinenko,[17] M.X. Liu,[27] Y. Liu,[36] C.F. Maguire,[49] Y.I. Makdisi,[5] A. Malakhov,[17] V.I. Manko,[23] Y. Mao,[7,38] G. Martinez,[45] M.D. Marx,[44] H. Masui,[48] F. Matathias,[44] T. Matsumoto,[8,50] P.L. McGaughey,[27] E. Melnikov,[15] F. Messer,[44] Y. Miake,[48] J. Milan,[43] T.E. Miller,[49] A. Milov,[44,51] S. Mioduszewski,[5] R.E. Mischke,[27] G.C. Mishra,[13] J.T. Mitchell,[5] A.K. Mohanty,[4] D.P. Morrison,[5] J.M. Moss,[27] F. Mühlbacher,[44] D. Mukhopadhyay,[51] M. Muniruzzaman,[6] J. Murata,[38,39] S. Nagamiya,[20] J.L. Nagle,[9] T. Nakamura,[14] B.K. Nandi,[6] M. Nara,[48] J. Newby,[46] P. Nilsson,[29] A.S. Nyanin,[23] J. Nystrand,[29] E. O'Brien,[5] C.A. Ogilvie,[16] H. Ohnishi,[5,38] I.D. Ojha,[49,3] K. Okada,[38] M. Ono,[48] V. Onuchin,[15] A. Oskarsson,[29] I. Otterlund,[29] K. Oyama,[8] K. Ozawa,[8] D. Pal,[51] A.P.T. Palounek,[27] V.S. Pantuev,[44] V. Papavassiliou,[34] J. Park,[42] A. Parmar,[33] S.F. Pate,[34] T. Peitzmann,[30] J.-C. Peng,[27] V. Peresedov,[17] C. Pinkenburg,[5] R.P. Pisani,[5] F. Plasil,[35] M.L. Purschke,[5] A.K. Purwar,[44] J. Rak,[16] I. Ravinovich,[51] K.F. Read,[35,46] M. Reuter,[44] K. Reygers,[30] V. Riabov,[37,40] Y. Riabov,[37] G. Roche,[28] A. Romana,[25] M. Rosati,[16] P. Rosnet,[28] S.S. Ryu,[52] M.E. Sadler,[1] N. Saito,[38,39] T. Sakaguchi,[8,50] M. Sakai,[32] S. Sakai,[48] V. Samsonov,[37] L. Sanfratello,[33] R. Santo,[30] H.D. Sato,[24,38] S. Sato,[5,48] S. Sawada,[20] Y. Schutz,[45] V. Semenov,[15] R. Seto,[6] M.R. Shaw,[1,27] T.K. Shea,[5] T.-A. Shibata,[47,38] K. Shigaki,[14,20] T. Shiina,[27] C.L. Silva,[41] D. Silvermyr,[27,29] K.S. Sim,[22] C.P. Singh,[3] V. Singh,[3] M. Sivertz,[5] A. Soldatov,[15] R.A. Soltz,[26] W.E. Sondheim,[27] S.P. Sorensen,[46] I.V. Sourikova,[5] F. Staley,[10] P.W. Stankus,[35] E. Stenlund,[29] M. Stepanov,[34] A. Ster,[21] S.P. Stoll,[5] T. Sugitate,[14] J.P. Sullivan,[27] E.M. Takagui,[41] A. Taketani,[38,39] M. Tamai,[50] K.H. Tanaka,[20] Y. Tanaka,[32] K. Tanida,[38] M.J. Tannenbaum,[5] P. Tarján,[11] J.D. Tepe,[1,27] T.L. Thomas,[33] J. Tojo,[24,38] H. Torii,[24,38] R.S. Towell,[1] I. Tserruya,[51] H. Tsuruoka,[48] S.K. Tuli,[3] H. Tydesjö,[29] N. Tyurin,[15] H.W. van Hecke,[27] J. Velkovska,[5,44] M. Velkovsky,[44] L. Villatte,[46] A.A. Vinogradov,[23] M.A. Volkov,[23] E. Vznuzdaev,[37] X.R. Wang,[13] Y. Watanabe,[38,39] S.N. White,[5] F.K. Wohn,[16] C.L. Woody,[5] W. Xie,[6] Y. Yang,[7] A. Yanovich,[15] S. Yokkaichi,[38,39] G.R. Young,[35] I.E. Yushmanov,[23] W.A. Zajc,[9,†] C. Zhang,[9] S. Zhou,[7] S.J. Zhou,[51] and L. Zolin[17]

(PHENIX Collaboration)

[1] *Abilene Christian University, Abilene, TX 79699, USA*
[2] *Institute of Physics, Academia Sinica, Taipei 11529, Taiwan*
[3] *Department of Physics, Banaras Hindu University, Varanasi 221005, India*
[4] *Bhabha Atomic Research Centre, Bombay 400 085, India*

[5]Brookhaven National Laboratory, Upton, NY 11973-5000, USA
[6]University of California - Riverside, Riverside, CA 92521, USA
[7]China Institute of Atomic Energy (CIAE), Beijing, People's Republic of China
[8]Center for Nuclear Study, Graduate School of Science, University of Tokyo, 7-3-1 Hongo, Bunkyo, Tokyo 113-0033, Japan
[9]Columbia University, New York, NY 10027 and Nevis Laboratories, Irvington, NY 10533, USA
[10]Dapnia, CEA Saclay, F-91191, Gif-sur-Yvette, France
[11]Debrecen University, H-4010 Debrecen, Egyetem tér 1, Hungary
[12]Florida State University, Tallahassee, FL 32306, USA
[13]Georgia State University, Atlanta, GA 30303, USA
[14]Hiroshima University, Kagamiyama, Higashi-Hiroshima 739-8526, Japan
[15]Institute for High Energy Physics (IHEP), Protvino, Russia
[16]Iowa State University, Ames, IA 50011, USA
[17]Joint Institute for Nuclear Research, 141980 Dubna, Moscow Region, Russia
[18]KAERI, Cyclotron Application Laboratory, Seoul, South Korea
[19]Kangnung National University, Kangnung 210-702, South Korea
[20]KEK, High Energy Accelerator Research Organization, Tsukuba-shi, Ibaraki-ken 305-0801, Japan
[21]KFKI Research Institute for Particle and Nuclear Physics (RMKI), H-1525 Budapest 114, POBox 49, Hungary
[22]Korea University, Seoul, 136-701, Korea
[23]Russian Research Center "Kurchatov Institute", Moscow, Russia
[24]Kyoto University, Kyoto 606, Japan
[25]Laboratoire Leprince-Ringuet, Ecole Polytechnique, CNRS-IN2P3, Route de Saclay, F-91128, Palaiseau, France
[26]Lawrence Livermore National Laboratory, Livermore, CA 94550, USA
[27]Los Alamos National Laboratory, Los Alamos, NM 87545, USA
[28]LPC, Université Blaise Pascal, CNRS-IN2P3, Clermont-Fd, 63177 Aubiere Cedex, France
[29]Department of Physics, Lund University, Box 118, SE-221 00 Lund, Sweden
[30]Institut für Kernphysik, University of Muenster, D-48149 Muenster, Germany
[31]Myongji University, Yongin, Kyonggido 449-728, Korea
[32]Nagasaki Institute of Applied Science, Nagasaki-shi, Nagasaki 851-0193, Japan
[33]University of New Mexico, Albuquerque, NM, USA
[34]New Mexico State University, Las Cruces, NM 88003, USA
[35]Oak Ridge National Laboratory, Oak Ridge, TN 37831, USA
[36]IPN-Orsay, Universite Paris Sud, CNRS-IN2P3, BP1, F-91406, Orsay, France
[37]PNPI, Petersburg Nuclear Physics Institute, Gatchina, Russia
[38]RIKEN (The Institute of Physical and Chemical Research), Wako, Saitama 351-0198, JAPAN
[39]RIKEN BNL Research Center, Brookhaven National Laboratory, Upton, NY 11973-5000, USA
[40]St. Petersburg State Technical University, St. Petersburg, Russia
[41]Universidade de São Paulo, Instituto de Física, Caixa Postal 66318, São Paulo CEP05315-970, Brazil
[42]System Electronics Laboratory, Seoul National University, Seoul, South Korea
[43]Chemistry Department, Stony Brook University, SUNY, Stony Brook, NY 11794-3400, USA
[44]Department of Physics and Astronomy, Stony Brook University, SUNY, Stony Brook, NY 11794, USA
[45]SUBATECH (Ecole des Mines de Nantes, CNRS-IN2P3, Université de Nantes) BP 20722 - 44307, Nantes, France
[46]University of Tennessee, Knoxville, TN 37996, USA
[47]Department of Physics, Tokyo Institute of Technology, Tokyo, 152-8551, Japan
[48]Institute of Physics, University of Tsukuba, Tsukuba, Ibaraki 305, Japan
[49]Vanderbilt University, Nashville, TN 37235, USA
[50]Waseda University, Advanced Research Institute for Science and Engineering, 17 Kikui-cho, Shinjuku-ku, Tokyo 162-0044, Japan
[51]Weizmann Institute, Rehovot 76100, Israel
[52]Yonsei University, IPAP, Seoul 120-749, Korea

(Dated: February 8, 2008)

Event-by-event fluctuations of the average transverse momentum of produced particles near mid-rapidity have been measured by the PHENIX Collaboration in $\sqrt{s_{NN}}$ = 200 GeV Au+Au and p+p collisions at the Relativistic Heavy Ion Collider. The fluctuations are observed to be in excess of the expectation for statistically independent particle emission for all centralities. The excess fluctuations exhibit a dependence on both the centrality of the collision and on the p_T range over which the average is calculated. Both the centrality and p_T dependence can be well reproduced by a simulation of random particle production with the addition of contributions from hard scattering processes.

PACS numbers: 25.75.Dw

The measurement of fluctuations in the event-by-event average transverse momentum of produced particles in

relativistic heavy ion collisions has been proposed as a probe of phase instabilities near the QCD phase transition [1, 2, 3], which could result in classes of events with different properties, such as the effective temperature of the collision. Fluctuation measurements could also provide information about the onset of thermalization in the system [4]. The resulting phenomena can be observed by measuring deviations of the event-by-event average p_T, referred to here as M_{p_T}, of produced charged particles from the expectation for statistically independent particle emission [5, 6] after subtracting contributions from fluctuations arising from physical processes such as elliptic flow and jet production.

Several M_{p_T} fluctuation measurements have been reported in heavy ion collisions [7, 8, 9, 10], including a study by PHENIX [9] in $\sqrt{s_{NN}} = 130$ GeV Au+Au collisions which set limits on the magnitude of non-random fluctuations in M_{p_T}. Recently, STAR has reported fluctuations in excess of the random expectation, within the PHENIX limits, at the same collision energy [10]. For the first results from $\sqrt{s_{NN}} = 200$ GeV Au+Au and p+p collisions reported here, upgrades of the PHENIX central arm spectrometers [11] have expanded the azimuthal acceptance from 58.5° to 180.0° within the pseudorapidity range of $|\eta| < 0.35$. Pad chamber and calorimeter detectors have also been utilized for improved background rejection. As a result, the sensitivity of the PHENIX spectrometer to the observation of fluctuations in M_{p_T} due to event-by-event fluctuations in the effective temperature [9, 12] has improved by greater than a factor of two.

Minimum bias events triggered by a coincidence between the Zero Degree Calorimeters (ZDC) and the Beam-Beam Counters (BBC), with a requirement that the collision vertex, which is measured with an r.m.s. resolution of less than 6 mm in central collisions and 8 mm in the most peripheral collisions, be within 5 cm of the nominal origin, are used in this analysis. Event centrality for Au+Au collisions, which is defined using correlations in the BBC and ZDC analog response [13], is divided into several classes, each containing an average of 244,000 analyzed events. These classes are associated to the estimated average number of participants in the collision, $< N_{part} >$, which is derived using a Glauber model Monte Carlo calculation with the BBC and ZDC detector response taken into account [14].

Charged particle momenta are reconstructed in the PHENIX central arm spectrometers with a drift chamber and a radially adjacent pixel pad chamber. Non-vertex track background rejection is provided by pixel pad chambers and calorimeters located further outward radially from the collision vertex [15]. The momentum resolution is $\frac{\delta p}{p} \simeq 0.7\% \oplus 1.0\% \times p$ (GeV/c).

M_{p_T} is calculated for each event, which contains a number of reconstructed tracks within a specified p_T range, N_{tracks}. The p_T range is always given a lower bound of 200 MeV/c and a varying upper bound, p_T^{max}, from 500 MeV/c to 2.0 GeV/c. There is a minimum N_{tracks} cut of 3 in both Au+Au events (removing 0%, 4.6%, and 29% of events in the 0-50%, 50-60%, and 60-70% centrality ranges, respectively, when $p_T^{max} = 2.0$ GeV/c) and p+p events (removing 59% of the events).

There are several measures by which the magnitude of non-random fluctuations can be quantified, namely ϕ_{p_T} [16, 17], $\nu_{dynamic}$ [18], and F_{p_T} [9]. The calculation of F_{p_T} is based upon the magnitude of the fluctuation, ω_{p_T}, defined as

$$\omega_{p_T} = \frac{(< M_{p_T}^2 > - < M_{p_T} >^2)^{1/2}}{< M_{p_T} >} = \frac{\sigma_{M_{p_T}}}{< M_{p_T} >}. \quad (1)$$

F_{p_T} is defined as the fractional deviation of ω_{p_T} from a baseline estimate defined using mixed events,

$$F_{p_T} = \frac{(\omega_{(p_T,\ data)} - \omega_{(p_T,\ mixed)})}{\omega_{(p_T,\ mixed)}}. \quad (2)$$

Mixed event M_{p_T} distributions are validated by comparisons to a calculation of M_{p_T} assuming statistically independent particle emission using parameters extracted from the inclusive p_T distributions of the data [19]. For the 0-5% centrality class, which suffers the most from tracking inefficiency, the effects of two-track resolution, and background contributions, the mixed event M_{p_T} distribution yields a value of $F_{p_T} = 0.04\%$ with respect to the calculation. The results of this comparison are included in the estimates of the systematic errors. Further details on the mixed event procedure and a discussion of contributions to the value of F_{p_T} from detector efficiency and resolution effects can be found in the description of the data analysis of $\sqrt{s_{NN}} = 130$ GeV Au+Au collisions [9].

Comparisons of the data and mixed event M_{p_T} distributions for the 0-5% and 30-35% centrality classes are shown in Fig. 1. Any excess fluctuations are small and are difficult to distinguish by eye in a direct overlay of the M_{p_T} distributions. Therefore, the comparison is also shown as residuals of the difference between the data and mixed event distributions in units of standard deviations of the individual data points. The double-peaked shape in the residual distributions is an artifact of the fact that the mixed event distributions, which always have a smaller standard deviation in M_{p_T} than the data, are normalized to minimize the total χ^2 of the residual distribution.

Figure 2 shows the magnitude of F_{p_T}, expressed in percent, as a function of centrality for Au+Au collisions with $p_T^{max} = 2.0$ GeV/c. The error bars are dominated by time-dependent systematic effects during the data taking period due to detector variations, which are minimized using strict time-dependent cuts on the mean and standard deviations of the inclusive p_T and N_{tracks} distributions. Statistical errors are below $F_{p_T} = 0.05\%$ for

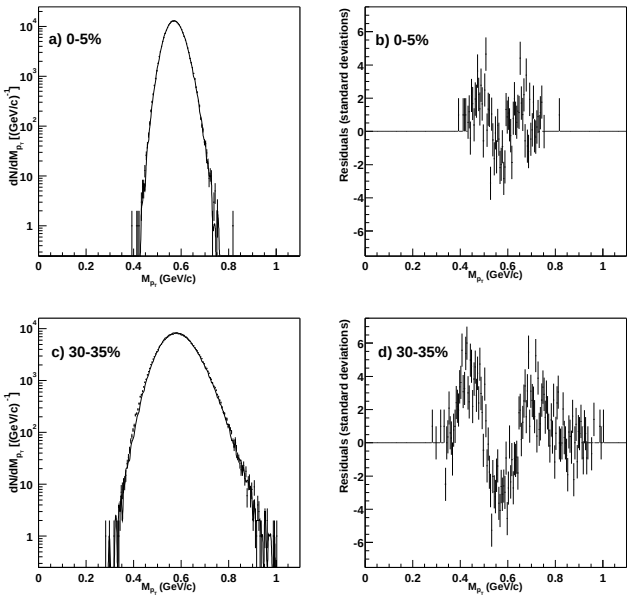

FIG. 1: Comparisons between the data and mixed event M_{p_T} distributions for the representative 0-5% and 30-35% centrality classes. Plots a) and c) show direct comparisons of the data (points) and normalized mixed event (solid line) M_{p_T} distributions. Plots b) and d) show the residuals between the data and mixed events in units of standard deviations of the data points from the mixed event points.

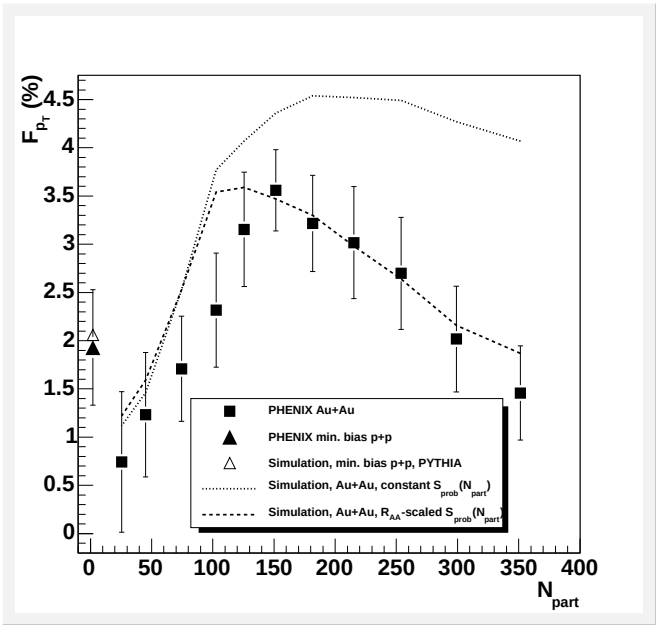

FIG. 2: F_{p_T} (in percent, 0.2 GeV/c $< p_T <$ 2.0 GeV/c) as a function of centrality, which is expressed in terms of the number of participants in the collision, N_{part}. The solid squares represent the Au+Au data. The solid triangle represents the minimum bias p+p data point. The open triangle is the result from an analysis of PYTHIA minimum bias p+p events within the PHENIX acceptance. The error bars include statistical and systematic errors and are dominated by the latter. The curves are the results of a Monte Carlo simulation with hard processes modelled using PYTHIA with a constant (dotted curve) and R_{AA}-scaled (dashed curve) hard scattering probability factor, and include the estimated contribution due to elliptic flow.

all centralities. The systematic errors are determined by dividing the entire dataset into ten separate subsets for each centrality class and extracting the standard deviation of the F_{p_T} values calculated for each subset. From Fig. 2, a significant non-random fluctuation is seen that appears to peak in mid-central collisions. However, the magnitude of the observed fluctuations are within previously published limits [9]. In addition, the value of F_{p_T} for the most peripheral Au+Au collisions is consistent with, albeit slightly below, the value measured by the same PHENIX apparatus in minimum bias $\sqrt{s_{NN}} = 200$ GeV p+p collisions. If the magnitude of F_{p_T} is entirely due to fluctuations in the effective temperature of the system [12], this measurement corresponds to a fluctuation of $\sigma_T / < T >$=1.8% at 0-5% centrality and 3.7% at 20-25% centrality.

To further understand the source of the non-random fluctuations, F_{p_T} is measured over a varying p_T range for which M_{p_T} is calculated, 0.2 GeV/c $< p_T < p_T^{max}$. Figure 3 shows F_{p_T} plotted as a function of p_T^{max} for the 20-25% centrality class. A trend of increasing F_{p_T} for increasing p_T^{max} is observed for this and all other centrality classes. The majority of the contribution to F_{p_T} appears to be due to correlations of particles with $p_T > 1.0$ GeV/c, where F_{p_T} increases disproportionately to the small increase (only 14%) of N_{tracks} in this region.

The behavior of F_{p_T} as a function of centrality and p_T is similar to trends seen in measurements of elliptic flow [20]. The contribution of elliptic flow to the magnitude of F_{p_T} is investigated using a Monte Carlo simulation whereby events are generated with a Gaussian distribution of N_{tracks} particles determined by a fit to the data and a random reaction plane azimuthal angle, Φ, between 0 and 2π. Independent particles within an event are generated following the inclusive p_T distribution with azimuthal angles, ϕ, distributed according to collective elliptic flow described by the function $\frac{dN}{d(\phi-\Phi)} = 1 + 2v_2 cos(2(\phi - \Phi))$. The values of the v_2 parameter are linearly parameterized as a function of p_T and centrality using PHENIX measurements of inclusive charged hadrons [20]. Only generated particles that lie within the PHENIX azimuthal acceptance are included in the calculation of M_{p_T}. This simulation estimates that the contribution of elliptic flow to F_{p_T} is largely cancelled out by the symmetry of the PHENIX acceptance, and is negligible for central collisions. The estimated elliptic flow contribution to the value of F_{p_T} is less than 0.1% for $N_{part} > 150$, increasing to about 0.6% for $N_{part} < 100$. Note that F_{p_T} measured for minimum

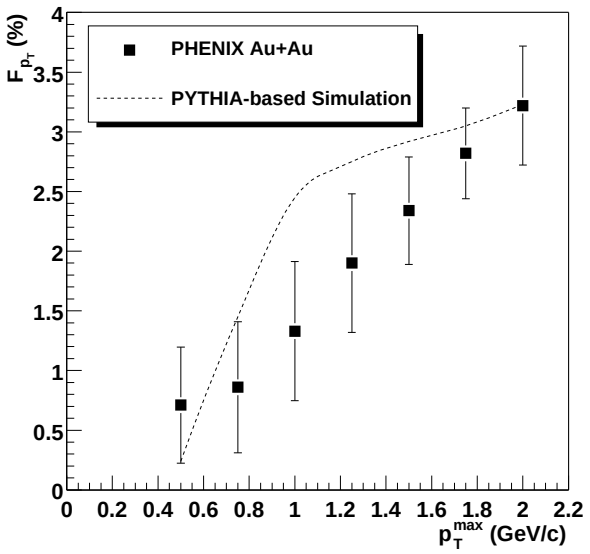

FIG. 3: F_{p_T} (in percent) of non-random fluctuations as a function of the p_T range over which M_{p_T} is calculated, 0.2 GeV/c $< p_T < p_T^{max}$, for the 20-25% centrality class (N_{part}=181.6). The curve is the result of a Monte Carlo simulation with hard-scattering processes modelled using PYTHIA with $S_{prob}(N_{part}) = 0.075$ and $R_{AA} = 0.41$ [23]. The error bars include statistical and systematic errors and are dominated by the latter. The contribution of elliptic flow is estimated to be negligible at this centrality.

bias p+p collisions, where collective flow is not expected to contribute, is non-zero ($1.9 \pm 0.6\%$), implying that a non-flow contribution may also be present in peripheral Au+Au collisions.

Figure 3 illustrates that a large contribution to the observed non-random fluctuations is due to the correlation of high p_T particles, such as might be expected from correlations due to jet production [21]. In order to estimate the contribution due to jets, a Monte Carlo simulation is again applied. Events are generated with a Gaussian distribution of N_{tracks} particles as independent particles that follow an m_T-exponential fit to the inclusive data p_T distribution. Hard processes are defined to occur at a uniform rate per generated particle, $S_{prob}(N_{part})$, for each centrality class. This is the only parameter that is allowed to vary in the simulation. As Au+Au events are being generated, single $\sqrt{s_{NN}} = 200$ GeV p+p hard-scattering events generated by the PYTHIA event generator [22] and filtered by the PHENIX acceptance are embedded into the event. The addition of the PYTHIA events affects the mean and standard deviation of the inclusive p_T spectra by less than 0.1%. The value of F_{p_T} has been extracted from 100,000 PYTHIA events for minimum bias p+p collisions, yielding F_{p_T}=2.06% within the PHENIX acceptance, which is consistent with the measured value of $F_{p_T} = 1.9 \pm 0.6\%$.

Two scenarios are considered for studies of the centrality-dependence of jet contributions to the value of F_{p_T}: 1) with $S_{prob}(N_{part})$ set at a constant rate for all centrality classes, and 2) with $S_{prob}(N_{part})$ scaled for each centrality class by the PHENIX measurement of the suppression of high p_T charged particles, which is characterized by the nuclear modification factor, R_{AA}, integrated over $p_T > 4.5$ GeV/c [23]. The p_T value at which R_{AA} is extracted has little effect on the simulation results, which change by less than 0.2% for 0-5% centrality if the R_{AA} measurement at $p_T = 2.0$ GeV/c is used instead. The latter scenario is intended to model the effect of the suppression of jets due to energy loss in the nuclear medium [24] on the fluctuation signal. The initial value of $S_{prob}(N_{part})$ for both scenarios is normalized so that the F_{p_T} result from the R_{AA}-scaled simulation matches that of the data for the 20-25% centrality class. The results of the simulation as a function of p_T^{max}, with $S_{prob}(N_{part})$ scaled by R_{AA}, are represented by the dashed curve in Fig. 3 for the 20-25% centrality class, The trend of increasing F_{p_T} with increasing p_T^{max} observed in the data is reproduced by the simulation reasonably well.

The results of the two hard scattering simulation scenarios are shown in Fig. 2 as a function of centrality. The model curves include the small contribution estimated from the elliptic flow simulation. The dotted curve is the result with $S_{prob}(N_{part})$ fixed for all centralities. The dashed curve is the result with $S_{prob}(N_{part})$ scaled by R_{AA} as a function of centrality. Within this simulation, the decrease of F_{p_T} for the more peripheral events is explained as a decrease in the signal strength relative to number fluctuations from the small and decreasing value of N_{tracks}. If $S_{prob}(N_{part})$ remains constant, the value of F_{p_T} decreases only slightly when going from mid-central to central collisions, in contradiction with the large decrease seen in the data over this centrality range. When $S_{prob}(N_{part})$ is scaled by R_{AA} as a function of centrality, the trend in the simulation of decreasing F_{p_T} with increasing centrality is more consistent with the data.

To summarize, the PHENIX experiment has observed a positive non-random fluctuation signal in event-by-event average transverse momentum, measured as a function of centrality and p_T in $\sqrt{s_{NN}} = 200$ GeV Au+Au and p+p collisions. The increase of F_{p_T} with increasing p_T implies that the majority of the fluctuations are due to correlated high p_T particles. A Monte Carlo simulation that includes elliptic flow and a PYTHIA-based hard scattering description can consistently describe contributions to the signal as a function of centrality and p_T with a simple implementation of jet suppression.

We thank the staff of the Collider-Accelerator and Physics Departments at BNL for their vital contributions. We acknowledge support from the Department of Energy and NSF (U.S.A.), MEXT and JSPS (Japan), CNPq and FAPESP (Brazil), NSFC (China), CNRS-

IN2P3 and CEA (France), BMBF, DAAD, and AvH (Germany), OTKA (Hungary), DAE and DST (India), ISF (Israel), KRF and CHEP (Korea), RMIST, RAS, and RMAE, (Russia), VR and KAW (Sweden), U.S. CRDF for the FSU, US-Hungarian NSF-OTKA-MTA, and US-Israel BSF.

---

* Deceased
† PHENIX Spokesperson:zajc@nevis.columbia.edu

[1] H. Heiselberg, Phys. Repts. **351**, 161 (2001).
[2] M. Stephanov *et al.*, Phys. Rev. Lett. **81**, 4816 (1998).
[3] M. Stephanov *et al.*, Phys. Rev. **D60**, 114028 (1999).
[4] S. Gavin, nucl-th/0308067, to be published.
[5] L. Stodolsky, Phys. Rev. Lett. **75**, 1044 (1995).
[6] E. Shuryak, Phys. Lett. **B423**, 9 (1998).
[7] NA49 Collaboration, H. Appelshäuser *et al.*, Phys. Lett. **B459**, 679 (1999).
[8] CERES Collaboration, D. Adamová *et al.*, Nucl. Phys. **A727**, 97 (2003).
[9] PHENIX Collaboration, K. Adcox *et al.*, Phys. Rev. **C66**, 024901 (2002).
[10] STAR Collaboration, preprint nucl-ex/0308033, to be published.
[11] PHENIX Collaboration, K. Adcox *et al.*, Nucl. Instrum. Methods **A499**, 235 (2003).
[12] R. Korus and S. Mrówczyński, Phys. Rev. **C64**, 054908 (2001).
[13] PHENIX Collaboration, K. Adcox *et al.*, Phys. Rev. Lett. **86**, 3500 (2001).
[14] PHENIX Collaboration, preprint nucl-ex/0307022, to be published.
[15] J. T. Mitchell *et al.*, Nucl. Instrum. Methods **A482**, 491 (2002).
[16] M. Gaździcki and S. Mrówczyński, Z. Phys. **C54**, 127 (1992).
[17] S. Mrówczyński, Phys. Lett. **B439**, 6 (1998).
[18] C. Pruneau *et al.*, Phys. Rev. **C66**, 044904 (2002).
[19] M. J. Tannenbaum, Phys. Lett. **B498**, 29 (2001).
[20] PHENIX Collaboration, S. S. Adler *et al.*, preprint nucl-ex/0305013, to be published; PHENIX Collaboration, K. Adcox *et al.*, Phys. Rev. Lett. **89**, 212301 (2002); STAR Collaboration, C. Adler *et al.* Phys. Rev. **C66**, 034904 (2002).
[21] Q. Liu and T. Trainor, Phys. Lett. **B567**, 184 (2003).
[22] T. Sjöstrand, Computer Physics Commun. **82**, 74 (1994). Version 5.720 with MSEL=1 for embedded hard scattering events and MSEL=2 for min. bias p+p events, CKIN(3)=0.0, MSTP(32)=4, and MSTP(33)=1.
[23] PHENIX Collaboration, preprint nucl-ex/0308006, to be published.
[24] X. N. Wang, Phys. Rev. **C58**, 2321 (1998).